

Experimental study of nucleate pool boiling of R134a on a stainless steel tube

Gerrit Barthau^{*}, Erich Hahne

Institut fuer Thermodynamik und Waermetechnik, University of Stuttgart, Pfaffenwaldring 6, D-70550 Stuttgart, Germany

Abstract

Nucleate pool boiling of R134a is studied experimentally in the reduced pressure range $0.03 \leq p/p_c \leq 0.5$ ($1.2 \text{ bar} \leq p \leq 20.3 \text{ bar}$) for heat fluxes from $q = 100\,000 \text{ W/m}^2$ down to single phase natural convection. Additionally to the heat transfer measurements, nucleation site density, up to $(N/A)_{\max} \approx 6000 \text{ sites/cm}^2$ is measured by an optical method. The test specimen is a horizontal stainless steel tube (sandblasted) with an outer diameter $d_o = 15.0 \text{ mm}$. The arrangement of the wall thermocouples allows for the direct measurement of the local radial heat flow. Experimental results: For the highest pressure investigated ($p/p_c = 0.5$) and for high heat fluxes ($q \geq 10\,000 \text{ W/m}^2$), the ratio of the local heat fluxes to the average heat flux is found to be in the range between 0.95 and 1.05, indicating that the boiling process around the test tube is only weakly influenced by the direction of the gravity field. For lower average heat fluxes, the angular heat flux variation increases, indicating the occurrence of two-phase convective effects. For the lower pressures, this convection dominated region extends to higher heat fluxes. The data for high heat fluxes (where nearly no angular variation occurs) are used for in situ evaluation of the thermal conductivity of the stainless steel wall material. The nucleation site density measurements are performed on the vertical flank of the test tube. The active nucleation sites are found to exhibit a rather strange behaviour on the sandblasted surface. Most of the sites emit only a series of few bubbles and then become inactive for a longer period; seldom a really stable nucleation site can be observed.

© 2003 Published by Elsevier Inc.

Keywords: Nucleate boiling; Natural convection; Angular heat flux distribution; Nucleation site density; R134a

1. Introduction

Experimental studies are still indispensable in the field of boiling heat transfer. Whereas for industrial applications increasingly more complex geometrical configurations and systems with unusual length scales have to be studied, for scientific research the most simple geometrical configurations—the horizontal plate and the horizontal tube—prevail. Probably due to experimental simplicity, many of the fundamental studies in boiling have been performed with horizontal tubes (see Gorenflo, 1994).

Precise wall temperature measurements in nucleate pool boiling experiments (e.g. Gorenflo et al., 2003) show a distinct angular variation of the local superheat. The superheat is found to be lowest at the bottom of the tube and highest at its top, its angular variation depending on (average) heat flux and also on reduced

pressure of the fluid. For evaluating the average superheat of the wall surface from the temperatures measured inside the wall, nearly always the average heat flux is used.

The present study deals with nucleate pool boiling heat transfer on a horizontal stainless steel tube with low thermal conductivity. A special arrangement of the wall thermocouples allows for the direct measurement of the angular distribution of the heat flux. According to the authors' knowledge, such experimental data are presented for the first time.

By definition, nucleate boiling is characterized by the formation of vapour bubbles from fixed sites randomly distributed on the heated surface. Consequently, the number of these sites per unit area, the active nucleation site density, is one of the key parameters in nucleate boiling. In one of the first basic studies of boiling, Jakob and Linke (1933) already counted active nucleation sites. An overview on further studies on nucleation site density is given by Barthau (1992). In all these studies it was found that nucleation site density increases with

^{*} Corresponding author. Fax: +49-711-685-3226.

E-mail address: barthau@itw.uni-stuttgart.de (G. Barthau).

increasing heat flux and nearly always it was tacitly assumed that sites, whenever activated, continue to emit bubbles at higher superheats and higher heat fluxes. Therefore, there was no demand for an explicit definition of the term “nucleation site density”. According to the authors’ knowledge, Judd and Merte (1970) were the first who clearly pointed out, that activated sites not continuously emit bubbles. To account for this, they defined an “average population density” and found in their experiments that the average population density is approximately one half the active site density for the same levels of heat flux and pressure. Barthau (1992) also found the ratio of the “momentary” nucleation site density and the “total” nucleation site density to be >0.5 on an emery ground horizontal copper tube. With the optical method developed in this study, total nucleation site densities up to 10 000 sites/cm² can be identified.

2. Experimental set-up

The test specimen is a horizontal stainless steel tube (material: W.Nr. 1.4301; AISI 304) with an outer diameter $d_o = 15$ mm and a length $l = 150$ mm. It is heated electrically by a cartridge heater which is shrunk centrically into the stainless steel tube. The cartridge heater has an outer diameter $d_c = 6.5$ mm, a heated length $l_h = 142$ mm and a maximum power $P_c = 1500$ W. To improve the fitting of the heater in the stainless steel tube, the bore of the tube was filled first with silver-bearing brazing alloy. To remove any flux contaminations and gas inclusions from the brazing alloy, the stainless steel tube was centrifuged when the liquid brazing alloy was filled in. The long bore for the cartridge heater can be machined more precisely and with a smoother surface in the brazing alloy than directly in the stainless steel.

The wall superheat $t_w - t_l$ is measured by 2×4 sheathed Ni–NiCr thermocouples (diameter: 0.5 mm) near the middle of the test tube (c.f. Fig. 1). The thermocouples are arranged equidistantly along the tube perimeter with nominal positions 0.9 and 2.8 mm respectively below the heating surface. After machining

the bores (by EDM), the actual position of the 8 bores relatively to the heating surface was measured with ± 0.02 mm accuracy.

The surface of the test tube was polished and then sandblasted. Its surface roughness was measured as $R_a = 0.18$ μm .

The wall superheat is measured directly against the liquid, i.e. the reference thermocouple is arranged in the liquid below the test tube.

The dc-power for the cartridge heater is voltage-controlled, the current is measured by the voltage drop of a calibrated high-precision resistor.

The temperatures of the fluid inside the boiling apparatus are measured with three calibrated multi-wire (cord) thermocouples. One of them is arranged in the liquid 30 mm below the test tube (together with the reference thermocouple for the wall superheat), the second one is arranged in the liquid 30 mm above the test tube, and the third one is arranged in the vapour space.

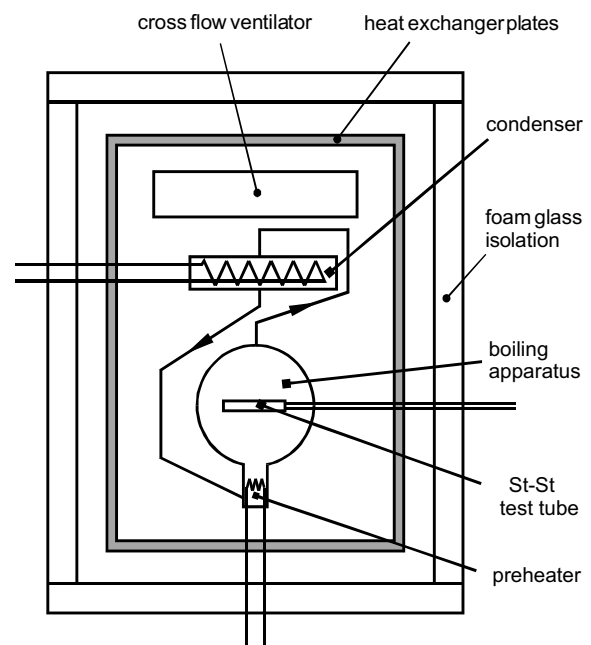


Fig. 2. Experimental set-up within temperature controlled cell.

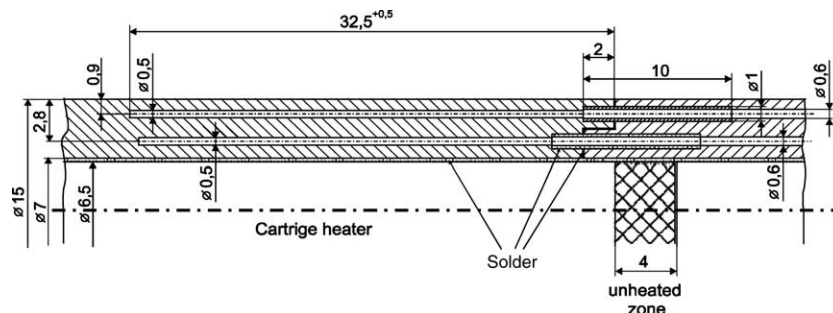


Fig. 1. Thermocouple-arrangement in the test-tube wall.

The stainless steel boiling apparatus (“German standard boiling apparatus”) is encased in a temperature controlled cell (c.f. Fig. 2). All walls of the cell consist of heat exchanger plates, therefore the internal heat flow in the cell is minimized.

Additionally, the air in the cell is circulated around the boiling apparatus by a large cross-flow ventilator. By adjusting the rotation speed of the ventilator, the temperature difference between the highest point of the boiling apparatus (the condenser) and its lowest point (the feed tube for the condensate) can be kept within $\Delta\vartheta_{\text{air}} = 0.02$ K. These temperatures are also measured with calibrated multi-wire thermocouples. Generally, the air temperature near the condenser is somewhat lower than the bottom temperature.

3. Experimental results and discussion

3.1. Average heat transfer coefficient

The experimental results for the heat transfer coefficient are shown in Fig. 3. For evaluating the heat transfer coefficient, the four local surface superheats were calculated from the measured superheats of the four thermocouples located 0.9 mm below the surface and then averaged arithmetically. The calculation of the surface superheats was performed with the directly measured local heat fluxes. The average heat flux q is evaluated from the measured electrical power and the heated tube length, assuming pure radial heat conduction and constant heat production of the cartridge heater along its heated length.

A comparison with heat transfer data for a gold-plated copper test tube with the same dimensions

(Barthau and Hahne, 2002) shows, that the average heat transfer coefficient of the stainless steel tube is somewhat lower. The differences are $\approx 25\%$ at the highest heat fluxes and $\approx 50\%$ at the lowest heat fluxes investigated.

3.2. Thermal conductivity of the stainless steel

For evaluating the surface temperature of the heating surface from the thermocouples inside the wall, the thermal conductivity of the wall material must be known. From Fig. 5 it is seen, that for high heat fluxes the ratio q_{loc}/q is ≈ 1 . When the average heat flow Q is known from the electrical input into the cartridge heater, from the 4 (nearly identical) radial temperature differences in the wall, the thermal conductivity of the stainless steel can be obtained. For this purpose only the data for which $0.95 \leq q_{\text{loc}}/q \leq 1.05$ have been used.

The results are presented in Fig. 4. The data show the common behaviour of stainless steel materials: a slight increase of the thermal conductivity with increasing temperature.

3.3. Angular distribution of the heat flux

The angular distribution of the heat flux is shown in Fig. 5. Here the ratio of the local heat flux q_{loc} to the average heat flux q is plotted vs. the average heat flux q .

For the highest reduced pressure $p/p_c = 0.5$ (Fig. 5(a)), at high heat fluxes ($q \geq 10000$ W/m²) the ratio $q_{\text{loc}}/q \approx 1$ is nearly the same in all directions (upward, downward and horizontal). This range, where the boiling process around the horizontal tube is nearly independent of the direction of the gravity field can be defined as “fully developed boiling”. Here, the nucle-

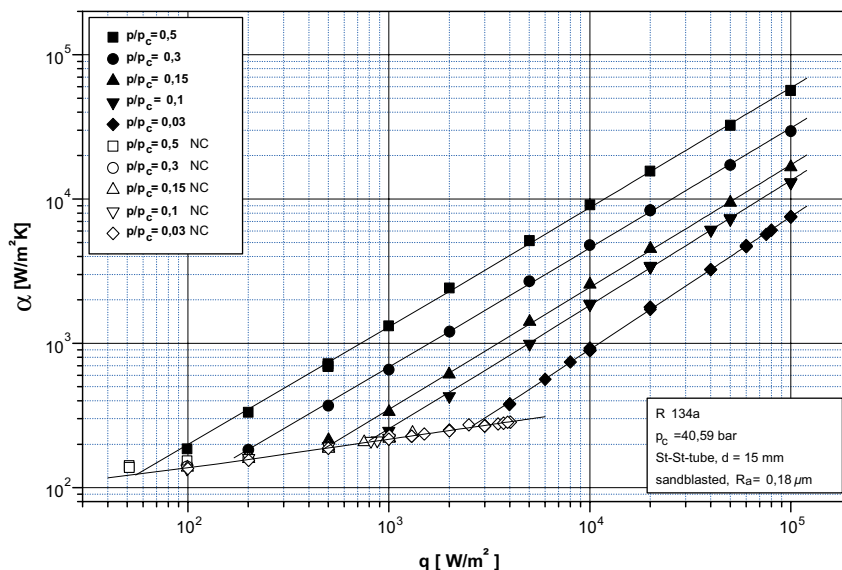


Fig. 3. Heat transfer coefficient α vs. heat flux q for different reduced pressures p/p_c .

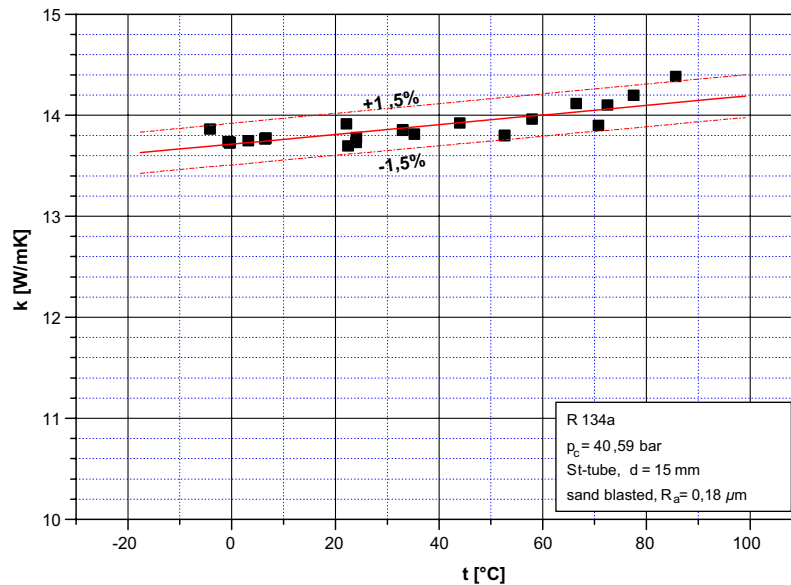


Fig. 4. Thermal conductivity k of the wall material (St-St, W.Nr. 1.4301; AISI 304).

ation site density seems to be so high, that the macroscopic two-phase flow around the tube is “blown away” from the tube’s surface. At lower heat fluxes, first q_{loc} in upward direction and then q_{loc} in downward direction become smaller than the average heat flux, whereas in the horizontal directions the local heat fluxes increase. This increase of the local heat flux at the flanks of the tube can be attributed to two-phase enhanced convection and/or to sliding bubble effects with increased latent heat transfer. Due to symmetry reasons, the local heat fluxes in horizontal direction (forward, backward) should be identical. The differences in the range $200 \text{ W/m}^2 \leq q \leq 1000 \text{ W/m}^2$ are thought to be caused by different nucleation site distributions on the heating surface near the thermocouples and not by measurement errors for the local heat fluxes.

For the lower pressures investigated, the fully developed boiling region becomes smaller (Figs. 5(b)–(d)).

For the lowest pressure ($p/p_c = 0.03$) it was possible to measure (with rising heat flux) single phase natural convection heat transfer (open symbols in Fig. 5) up to heat fluxes $q \approx 4000 \text{ W/m}^2$. For the boiling runs (performed with decreasing heat flux) the local boiling heat fluxes have to merge with the single phase natural convection heat fluxes when the heat flux becomes smaller and smaller and when the nucleation site density decreases and finally becomes $N/A = 0$. This merging can be seen most clearly in Fig. 5(e).

3.4. Angular distribution of the heat transfer coefficient

The angular distribution of the heat transfer coefficient is shown in Fig. 6. The ratio of the local heat

transfer coefficient α_{loc} (evaluated with the *local* superheat) to the average heat transfer coefficient α is plotted vs. the (average) heat flux q .

From Fig. 6(e) it is seen that for single phase natural convection the ratio α_{loc}/α is independent of heat flux. The heat transfer coefficient is highest at the bottom and lowest at the top of the tube.

In the boiling region, for all pressures at high heat fluxes α_{loc} is highest at the bottom. When the heat flux decreases, $\alpha_{loc, bottom}$ reaches a minimum value and then increases again to merge with the single phase natural convection data.

From Figs. 6(a)–(d) some conclusions concerning the experimental uncertainty can be drawn. Due to symmetry reasons, the heat transfer coefficients at the flanks of the tube should be identical for the fully developed boiling regime, where the nucleation site density is very high. As can be seen, the difference between the forward and the backward α_{loc} increases with increasing heat flux, the difference being most pronounced at the highest pressure $p/p_c = 0.5$ where the superheat of the heating surface is smallest. The superheat is evaluated from the temperatures measured inside the wall assuming a logarithmic temperature profile. However, due to the small distances involved (nominally about 0.9 mm), the error in the evaluated superheat due to a position error of the thermocouple junction and therewith the error of the corresponding heat transfer coefficient should grow nearly linearly with the heat flux. Fig. 6 shows that for high heat fluxes ($q > 10^4 \text{ W/m}^2$) this condition mainly holds for the backward heat transfer coefficient (diamond symbol). For $q = 100000 \text{ W/m}^2$ the temperature gradient in the stainless steel tube wall near the surface is about 8 K/mm. Therefore a position error of the junc-

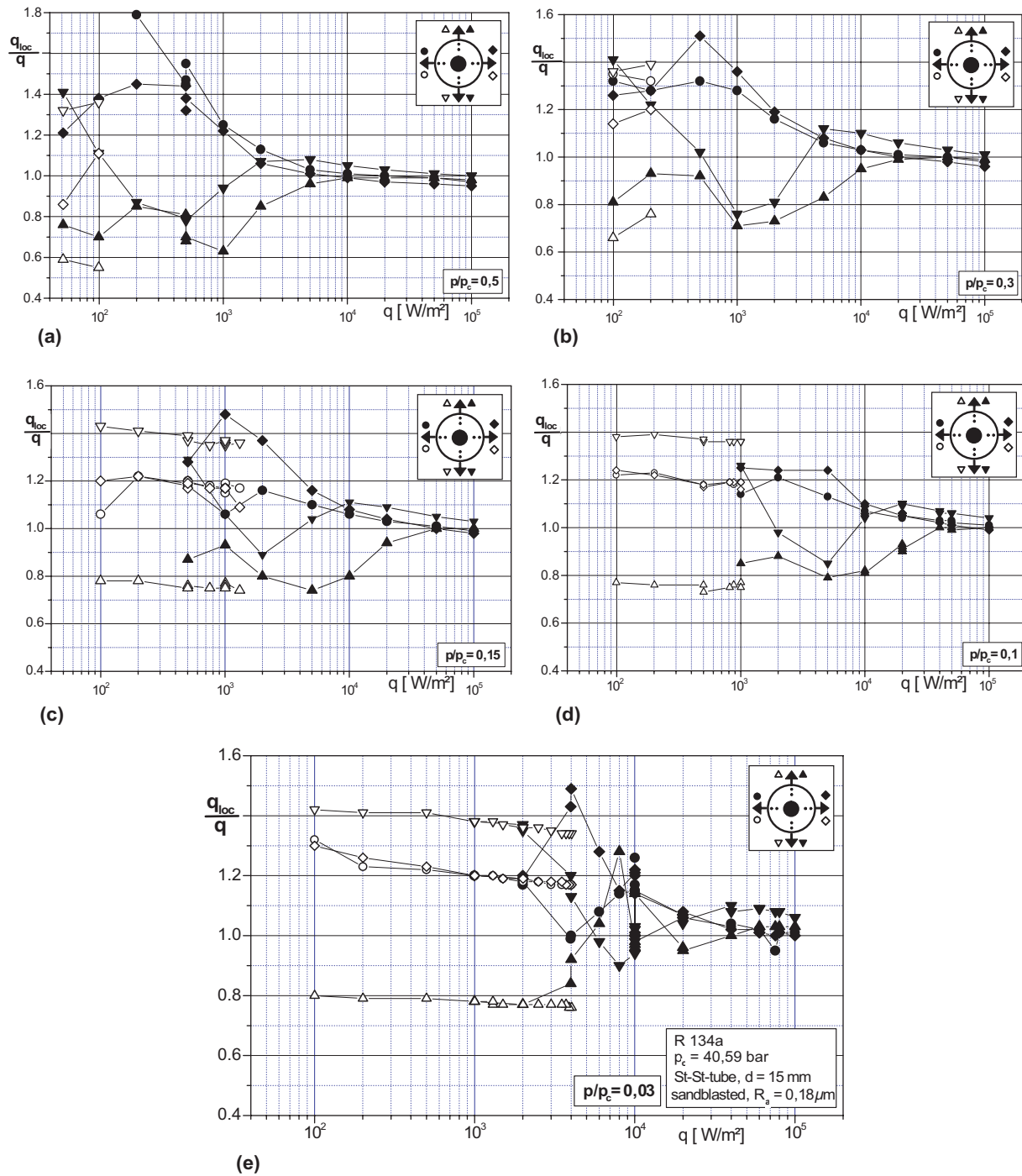


Fig. 5. Ratio of the local heat flux q_{loc} to the heat flux q vs. heat flux q for different reduced pressures p/p_c .

tion in the sheathed (backward) thermocouple of less than 0.1 mm could account for the difference of the measured local heat transfer coefficients in the high heat flux region. Additionally it should be kept in mind that there is a temperature gradient across the thermocouples junction whose diameter is estimated to be about 0.15 mm.

For decreasing pressures, the superheat at constant heat flux increases and therefore the corresponding relative error for α_{loc} becomes smaller.

The strong increase of the local heat transfer coefficient at the bottom of the tube at the highest heat fluxes for $p/p_c = 0.5$ cannot be attributed uniquely to a position error of the junction of the respective

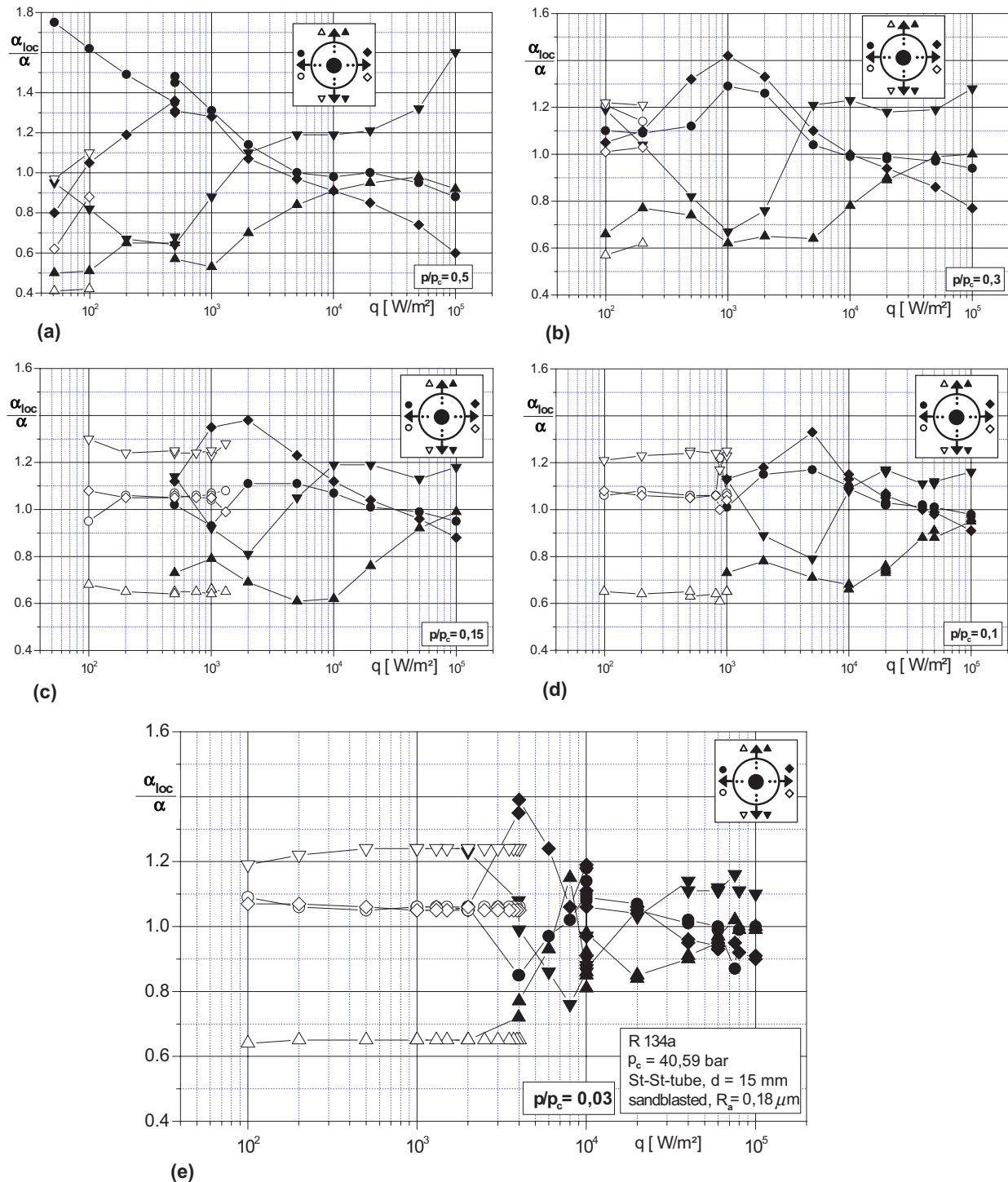


Fig. 6. Ratio of the local heat transfer coefficient α_{loc} to the heat transfer coefficient α vs. heat flux q for different reduced pressures p/p_c .

thermocouple. As can be seen from Figs. 6(b)–(d), the relative deviation of the bottom heat transfer coefficient does not change monotonously with heat flux, as would be typical for a position error.

For heat fluxes $q < 10^4$ W/m², the influence of possible position errors of the thermocouple junctions becomes nearly negligible. As long as the forward and backward

heat transfer coefficients are nearly identical, the angular distribution of the heat transfer coefficient is thought to be governed mainly by the two-phase natural convection flow (including sliding bubble effects) around the tube. This range is most extended at the high pressures.

When at low heat fluxes the difference between forward and backward heat transfer coefficients increases,

this is thought to be due to the local random distribution of the nucleation sites near the respective thermocouples at now rather low nucleation site densities.

When the nucleation site density approaches $N/A = 0 \text{ cm}^{-2}$, the boiling heat transfer coefficients have to merge with the single phase natural circulation ones.

3.5. Nucleation site density

The nucleation site density has been measured at the vertical flank of the test tube (i.e. at the horizontal forward position near the respective thermocouple) with an optical method (see Barthau, 1992). In Fig. 7, data are shown for the “total” nucleation site density $(N/A)_{\text{tot}}$ and the “momentary” nucleation site density $(N/A)_{\text{mom}}$.

The total nucleation site density is defined as the number of points per unit area of the heating surface, which can emit bubbles at a given pressure and at a given heat flux. The momentary nucleation site density is defined as the number of sites per unit area which are active at a given “moment”. It makes sense to choose the “duration of the moment” in the range of the growth time of a bubble.

The nucleation site density has been measured using a CCD-camera (with different optical magnifications, shutter time: 1/60 s) and a standard video recorder, which records 50 “half-frames”/s.

For measuring the total nucleation site density, a video sequence of about 20 s length has been analysed.

For evaluating the momentary nucleation site density, the number of bubbles attached to the surface (and visible as “dark spots”) was counted in about 15 consecutive frames and then averaged.

As can be seen from Fig. 7, $(N/A)_{\text{tot}}$ is about two orders of magnitude higher than $(N/A)_{\text{mom}}$ for

$p/p_c = 0.5$ and about one order of magnitude for $p/p_c = 0.03$.

Similar behaviour has been found by Barthau and Hahne (2001) and by Gorenflo et al. (2003) in studies performed also with sandblasted tubes. This unusual behaviour of the nucleation sites seems to be characteristic of sandblasted surfaces, indicating that such surfaces offer much more cavities of a given size range than can be provided with heat and then can actually lead to nucleation.

According to our knowledge, Judd and Merte (1970) were the first to point out that $(N/A)_{\text{mom}}$ and $(N/A)_{\text{tot}}$ are not identical; they found $(N/A)_{\text{mom}}/(N/A)_{\text{tot}} \approx 0.5$ for pool boiling of subcooled water. Barthau (1992) and Barthau and Hahne (2000) also measured $0.5 \leq (N/A)_{\text{mom}}/(N/A)_{\text{tot}} \leq 1$ on sanded copper surfaces with boiling of R114 and R134a.

The sanded copper test-tube used in the study of Barthau and Hahne (2000) and the stainless steel test-tube used in the present study have the same geometrical dimensions. It is very interesting to note, that the heat transfer coefficients on both tubes differ by less than 30% for R134a, whereas the nucleation site behaviour is totally different.

4. Conclusions

The arrangement of “double thermocouples” in the wall of the test tube proved to be successful. The possibility to measure in situ the thermal conductivity of the wall material improves the reliability of the experimental heat transfer data. According to the authors’ knowledge, such experimental data are presented for the first time.

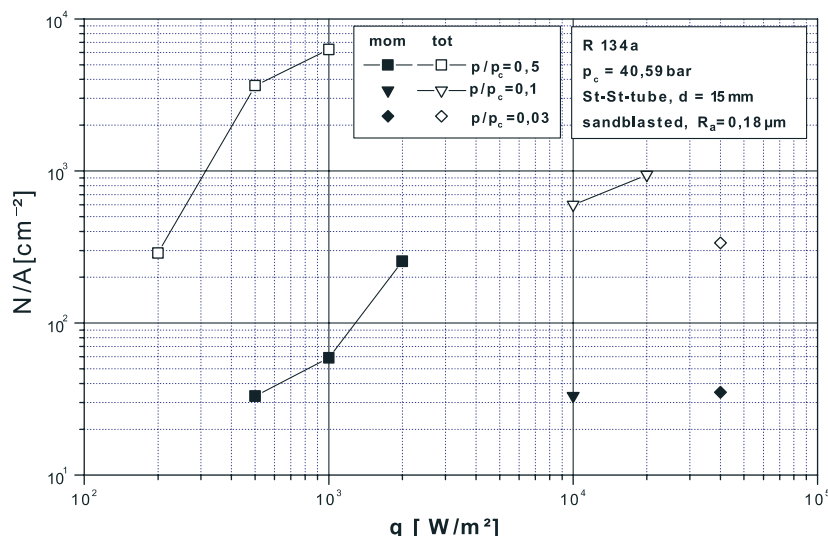


Fig. 7. Nucleation site density N/A vs. heat flux q for different reduced pressures p/p_c .

The heat flux and the heat transfer distributions around a horizontal tube are rather complicated, depending on pressure and average heat flux as shown in Figs. 5 and 6. At least three different boiling-ranges can be identified on the basis of the new experimental data: At high heat fluxes, the local heat flux behaves radial-symmetric, i.e. it is independent of the direction of the gravity field. At lower heat fluxes, the angular local heat flux distribution seems to be governed by the macroscopic two-phase flow around the tube. At even lower average heat fluxes (and therefore low nucleation site densities) the local heat fluxes seem to be governed also by the random distribution of the active nucleation sites. These results might be influential on future boiling models. Nucleate pool boiling around a horizontal tube is to be seen as a conjugated, inverse heat transfer problem.

At least on sandblasted surfaces, the concept of evaluating boiling heat transfer on the basis of nucleation site density, becomes questionable.

Acknowledgements

The authors highly appreciate financial support of Deutsche Forschungsgemeinschaft in the frame of a Joint German Research Project on fundamentals of boiling heat transfer. The finishing of the test tubes surface, the roughness measurement and the measure-

ment of the surface topography has been accomplished by Dr.-Ing. habil. Andrea Luke, WKT, University Paderborn as part of this project. The high purity test liquid was supplied by Solvay company. The authors gratefully acknowledge this support.

References

- Barthau, G., 1992. Active nucleation site density and pool boiling heat transfer—an experimental study. *Int. J. Heat Mass Transfer* 35, 271–278.
- Barthau, G., Hahne, E., 2000. Nucleation site density and heat transfer in nucleate pool boiling of refrigerant R134a in a wide pressure range. In: 3rd European Thermal-Sciences Conference, Heidelberg, vol. 2, pp. 731–736.
- Barthau, G., Hahne, E., 2001. Nucleate pool boiling of refrigerant R 134a on a gold-plated copper test tube. IIF–IIR-Commission-B1-Paderborn, Germany-2001/5.
- Barthau, G., Hahne, E., 2002. Second order effects in an experimental study of nucleate pool boiling of R134a. In: 12th Int. Heat Transfer Conf. Grenoble, France, vol. 3, p. 683.
- Gorenflo, D., 1994. Behaeltersieden (Sieden bei freier Konvektion). VDI-Waermeatlas, 7.Auflage, Hab 1.
- Gorenflo, D., Danger, E., Luke, A., Kotthoff, S., Chandra, U., Ranganayakulu, C., 2003. Bubble formation with pool boiling on tubes with or without basic surface modifications for enhancement. In: 5th Int. Conf. Boiling Heat Transfer, Montego Bay, Jamaica.
- Jakob, M., Linke, W., 1933. Der Wärmeübergang von einer waagerechten Platte an siedendes Wasser. *Forsch. Ing. Wes.* 4, 75–81.
- Judd, R.L., Merte, H., 1970. Influence of acceleration on subcooled nucleate pool boiling. In: 4th Int. Heat Transfer Conf., Paris–Versailles, vol. 6, p. B8.7.